Journal of Nuclear Cardiology (xxxx) xxx, xxx

ORIGINAL RESEARCH

Folate receptor β-targeted Positron emission tomography imaging of activated macrophages in experimental myocardial infarction

Imran Iqbal, PharmD, MSc [1], Heidi Liljenbäck, MSc [1,2], Putri Andriana, PhD [1], Mia Ståhle, PhD [1], Jenni Virta, PhD [1], Erika Atencio Herre, MSc [1], Maxwell W.G. Miner, PhD [1], Arman Anand, MBBS, MSc [1], Aino Suni, MSc [1], Wail Nammas, MD [1,3], Ville Kytö, MD, PhD [1,4], Hasan Mansour A Mansour, BSc [5], Nathan A. Cleveland, BSc [5], Xiang-Guo Li, PhD [1,6,7], Madduri Srinivasarao, PhD [5], Philip S. Low, PhD [5], Juhani Knuuti, MD, PhD [1,7], Anne Roivainen, PhD [1,2,7], Antti Saraste, MD, PhD [1,3,7,*]

[1] Turku PET Centre, University of Turku and Turku University Hospital, Turku, Finland
[2] Turku Center for Disease Modeling, University of Turku, Turku, Finland
[3] Heart Center, Turku University Hospital and University of Turku, Turku, Finland
[4] Turku Clinical Research Center, Turku University Hospital and University of Turku, Turku, Finland
[5] Department of Chemistry, Purdue University, West Lafayette, USA
[6] Department of Chemistry, University of Turku, Turku, Finland
[7] InFlames Research Flagship, University of Turku, Turku, Finland

[*] Corresponding author. Heart Center, Turku University Hospital, Turku, Finland.
E-mail address: antti.saraste@utu.fi (Antti Saraste).

Abstract

Background: Folate receptor β (FR-β) is expressed on activated macrophages in inflammatory conditions. In order to study FR-β in inflammatory response following myocardial infarction (MI), we evaluated FR-β-targeted PET imaging using aluminum fluoride-18-labeled NOTA-folate ([^{18}F]FOL) in a rat model of MI.

Methods: Rats underwent [^{18}F]FOL PET imaging on 3, 7, 15, and 90 days after induction of MI by permanent coronary artery ligation or sham operation. [^{18}F]FDG PET was performed a day before [^{18}F]FOL scans to localize the infarct area. A subset of rats underwent [^{18}F]FOL PET on day 7 and serial echocardiography until 90 days post-surgery.

Results: The [^{18}F]FOL uptake was significantly higher in the infarct area than in the myocardium of sham-operated rats on day 3 (SUV 1.97 ± 0.17 vs 0.74 ± 0.13), and remained higher on day 7 (SUV 1.35 ± 0.33 vs 0.70 ± 0.16), day 15 (SUV 1.24 ± 0.20 vs 0.59 ± 0.07), and day 90 (SUV 1.39 ± 0.25 vs 0.69 ± 0.11). Autoradiography of tissue sections confirmed tracer uptake in the infarct area, where immunofluorescence showed FR-β in CD68-positive macrophages. Uptake of [^{18}F]FOL correlated with CD68-positive macrophage density ($r = 0.669$, $P < 0.001$) and was associated with decline in left ventricular ejection fraction between days 7 and 90 post-MI ($r = -0.665$, $P = 0.007$).

Conclusion: [^{18}F]FOL PET detects expression of FR-β, a marker of activated macrophages after MI. FR-β expression peaks early and remains elevated up to 3 months post-MI. Early FR-β expression is associated with worsening of left ventricular systolic function.

Received 30 June 2025; Accepted 24 January 2026; Available online XXX

https://doi.org/10.1016/j.nuclcard.2026.102653

Keywords: Macrophage, Myocardial infarction, PET, Folate receptor β, Ejection fraction, Rat

ABBREVIATIONS

FR-β	Folate receptor beta
PET	Positron emission tomography
[^{18}F]FOL	Aluminum fluoride-18-labeled 1,4,7-triazacyclononane-1,4,7-triacetic acid conjugated folate
[^{18}F]FDG	Fluoride-18-labelled fluorodeoxyglucose
MI	Myocardial infarction
SUV	Standardized uptake value
LV	Left ventricle
LVEF	Left ventricular ejection fraction
LVSvol(i)	Left ventricular end systolic volume index to body weight
LVDvol(i)	Left ventricular end diastolic volume index to body weight

INTRODUCTION

Macrophages are key cells that determine the balance between pro-inflammatory and anti-inflammatory responses after myocardial infarction (MI) [1,2]. An imbalanced and/or prolonged inflammation can contribute to incomplete scar healing, adverse left ventricular (LV) remodeling, compromised LV function, and eventually chronic heart failure [1,3]. The pro-inflammatory response, associated with classically activated macrophages, peaks early after MI followed by suppression of inflammation associated with alternatively activated macrophages. These macrophage subtypes can be distinguished based on their surface receptors or cytokines they release [1,4,5]. Among other cell surface receptors, activated macrophages also express folate receptor beta (FR-β), a glycosylphosphatidylinositol-anchored membrane protein, which binds to folate ligands with high affinity and internalizes them via endocytosis [6–8]. However, the role of FR-ß in the inflammatory response with respect to MI is unknown.

PET tracers targeting cell surface markers of leukocyte subpopulations have been studied to obtain information about the inflammatory response following MI [9]. Previously, it has been shown that FR-β-targeted PET with aluminum fluoride-18-labeled 1,4,7-triazacyclononane-1,4,7-triacetic acid conjugated folate ([^{18}F]FOL) detects active inflammation associated with autoimmune myocarditis [10], atherosclerosis [11], and neuroinflammation [12]. More recently, uptake of [^{18}F]FOL was demonstrated after experimental MI [13].

This study evaluates FR-β-targeted [^{18}F]FOL PET to investigate the inflammatory response post-MI. We studied myocardial uptake of [^{18}F]FOL by PET and tissue samples at different time-points after coronary ligation as well as relationships between the uptake of [^{18}F]FOL, inflammation, and LV function in a rat model of MI.

METHODS

Supplementary methods are available at https://www.journalofnuclearcardiology.org/

ANIMAL MODEL AND STUDY DESIGN

MI was induced by surgical ligation of the left coronary artery in 7–9-week-old male Sprague-Dawley rats as described previously [14,15]. Sham operation included all the steps of the surgical procedure except the LCA ligation. The animal studies were approved by the national Project Authorization Board (ESAVI/43134/2019) in Finland.

PET

The rats underwent a [^{18}F]FOL PET scan on days 3, 7, 15 or 90 post-MI or sham-operation with a dedicated small animal device (Inveon Multimodality; Siemens Medical Solutions, Knoxville, TN, USA) under isoflurane anesthesia (4%–5% induction, 1.5%–2% maintenance) as described earlier [14,15]. The numbers of animals are shown in Supplementary Table 1. Except for day 15, the rats underwent fluoride-18-labeled fluorodeoxyglucose ([^{18}F]FDG) PET one day before [^{18}F]FOL PET for localization of the heart and infarct area. A computed tomography (CT) scan was performed before each PET scan for attenuation correction. A 10-min static PET acquisition, starting 10 minutes after the intravenous injection of [^{18}F]FDG (33.73 ± 4.13 MBq) and either a 60-min dynamic PET acquisition (n = 2 rats with MI on day 3 and n = 4 on day 7) or a 20-min static PET acquisition starting 20 minutes after the intravenous injection of [^{18}F]FOL (49.22 ± 5.66 MBq) were performed. The PET data acquired were reconstructed using 2

iterations with 3-dimensional ordered-subsets expectation maximization and 18 maximum a posteriori iterations algorithms.

PET images were analyzed using Carimas v.2.10 software (Turku PET Centre, Turku, Finland) without performing a partial-volume correction. After manual co-registration of the [^{18}F]FDG and [^{18}F]FOL images, the regions of interest were defined based on myocardial contours in the [^{18}F]FDG image in the infarct area showing focally reduced [^{18}F]FDG uptake or corresponding area in sham-operated rats, remote myocardium in the interventricular septum, LV blood pool, liver, lungs, and surgical wound area in the chest wall. Tracer uptake kinetics were visualized as time-activity curves in dynamic scans as described previously [14,15]. Standardized uptake values (SUVs) were calculated as the mean radioactivity concentration (Becquerel per milliliter or kBq/mL) divided by the injected radioactivity dose normalized for body weight. In a subgroup of rats undergoing serial echocardiography, MI size on day 7 was measured in [^{18}F]FDG polar maps as myocardium showing <70% tracer uptake of the maximum uptake.

ECHOCARDIOGRAPHY

Function of the LV was evaluated by a dedicated small animal ultrasound device (Vevo 2100, VisualSonics, Inc., Toronto, ON, Canada) in a subgroup of rats, which underwent [^{18}F]FOL PET on day 7 and serial echocardiography on days 7, 15, and 90 post-MI ($n = 15$) or sham-operation ($n = 5$) as described previously [14,15]. Parasternal long-axis 2D images were obtained to measure LV ejection fraction (LVEF), LV diastolic and systolic volumes indexed to body weight (LVDvol(i), LVSvol(i) respectively).

EX VIVO BIODISTRIBUTION OF [^{18}F]FOL

The evaluation of ex vivo biodistribution of [^{18}F]FOL approximately 65 minutes after injection was performed in organs as shown in the Supplementary Table 2.

AUTORADIOGRAPHY, HISTOLOGY, AND IMMUNOSTAINING

The LV was frozen in dry-ice-cooled isopentane, and cut into serial 8 μm and 20 μm thick transverse cryosections at 1-mm intervals from base to apex. Myocardial uptake of [^{18}F]FOL was investigated ex vivo by performing digital autoradiography of LV cryosections of 20 μm thickness. Sections were briefly air-dried, slides placed on imaging plates (Fuji Imaging Plate BAS-TR2025, Fuji Photo Film Co. Tokyo, Japan), and exposed for approximately four hours. Imaging plates were then scanned with Fuji BAS-5000 analyzer at internal resolution of 25 μm. Sections were stained with hematoxylin and eosin (H&E), scanned with a digital slide scanner (Pannoramic P1000, 3DHistech Ltd., Budapest, Hungary), and superimposed with autoradiographs. Multiple ROIs were defined after co-registration of histological images and autoradiographs in both infarct and remote areas in 10 to 14 sections per heart. Results were corrected for background radioactivity, and calculated as photostimulated luminescence per square millimeter (PSL/mm^2) with TINA software version 2.10f (Raytest Isotopenmeβgeräte, GmbH, Straubenhardt, Germany). Results were decay-corrected for injection and exposure times, and normalized for injected radioactivity dose.

Size of the MI was measured in hematoxylin-eosin (H&E) stained sections as the average percentage of LV circumference as described previously [13–15]. Macrophages were detected by immunohistochemical staining using mouse monoclonal anti-rat CD68 antibody in LV cryosections of 8 μm thickness as described previously [15]. Sections were scanned with a digital slide scanner and percentage area of myocardium positive for CD68 within infarct area or remote myocardium was measured in 10 to 12 sections per heart using Image-J (version 1.46) software (National Institute of Health, Bethesda, MD, USA) and specific color threshold values. Additional immunohistochemical stainings with antibodies against inducible nitric oxide synthase (iNOS), mannose receptor C-type 1 (MRC-1) and FR-β were performed in formalin –fixed, paraffin-embedded sections of 4 μm thickness to detect the presence of M1-and M2-type macrophages and FR-β, respectively [10,16]. To evaluate co-localization of FR-β and CD68-positive macrophages, double immunofluorescence staining was performed on formalin-fixed, paraffin-embedded sections of 4 μm thickness [10,11] (Supplementary Table 3).

EFFECT OF FOLATE GLUCOSAMINE ON THE UPTAKE OF [^{18}F]FOL

The specificity of the uptake of [^{18}F]FOL was studied in 3 rats 3 days after MI. PET and ex vivo analyses were performed as described above, except that a 100-fold molar excess of folate glucosamine ($C_{25}H_{30}N_{10}$; 100 μL) binding to FR-β was injected intravenously 10 minutes before [^{18}F]FOL injection.

STATISTICAL ANALYSIS

Continuous data were reported as mean and standard deviation, and compared using Student's *t*-test. One-way analysis of variance followed by Tukey's honestly significant difference

test was used for comparisons of multiple time-points. Spearman's rank correlation coefficient was determined to analyze the correlation between two continuous variables. A linear regression model adjusted for MI size was constructed to evaluate the association between [^{18}F]FOL uptake in the infarct area and the change in LV function at follow-up. A *P*-value of less than 0.05 was considered statistically significant. Statistical analyses were performed using MS Excel 2016 (Microsoft Corporation, USA) and SPSS (version: 28.0.1.0 (142), IBM Statistics, NY, USA).

RESULTS

Histology of myocardial infarction

Histological analysis of all LCA-ligated rats showed the presence of MI on days 3, 7, and 90 (Figures 1A and 2A). Average size of the MI was 42.2% ± 11.45, 40.4% ± 10.38, and 45.5% ± 7.00 of the LV on days 3, 7 and 90, respectively. There were no infarctions in sham-operated rats.

The amount of CD68-positive macrophages in the infarct area peaked on day 3 and remained higher compared to sham-operated rats on day 7 and day 90 with consistent *P*-value of <0.001 at all time points. In the remote myocardium, few CD68-positive cells were present, with a transient increase on day 3 in MI versus sham-operated rats ($P < 0.017$) (Figure 1B).

In the infarct area, immunohistochemical staining showed the presence FR-β-positive cells, MRC-1-positive cells, indicating presence of anti-inflammatory macrophages, and some iNOS-positive staining, indicating presence of pro-inflammatory macrophages, at all time points (Figure 2A). Double immunofluorescence staining demonstrated FR-β expression in a large proportion of CD68-positive macrophages within the infarct area at all time-points (Figure 2B). Furthermore, scattered FR-β-positive macrophages were also observed in regions outside the infarct area (Supplementary Fig. 1).

In vivo PET/CT imaging of FR-β

[^{18}F]FOL PET showed visually increased uptake of the radiotracer in the area corresponding to the

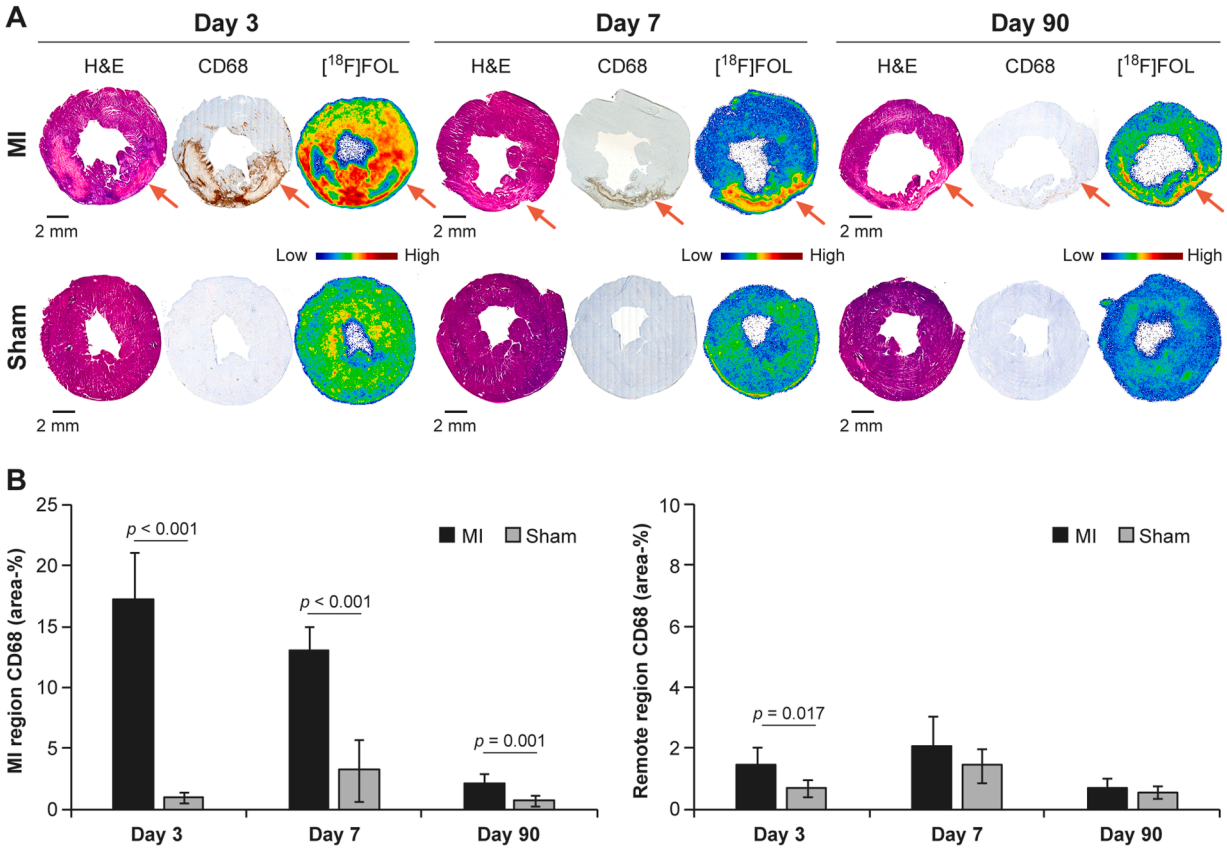

Figure 1. Histology and [^{18}F]FOL autoradiography. (A) Hematoxylin and eosin (H&E) staining, CD68 immunohistochemistry, and an ex vivo autoradiography of [^{18}F]FOL uptake on days 3, 7, and 90 after myocardial infarction (MI) or sham operation in representative LV short-axis tissue sections. The uptake of [^{18}F]FOL co-localizes with CD68-positive macrophages in the infarct area (arrows), extending to adjacent areas on day 3. (B) Area percentage of CD68-positive macrophages is higher in infarct area than myocardium of sham-operated rats on days 3, 7, and 90. In the remote area, CD68-positive staining transiently increases on day 3. Numbers of animals are shown in Supplementary Table 1.

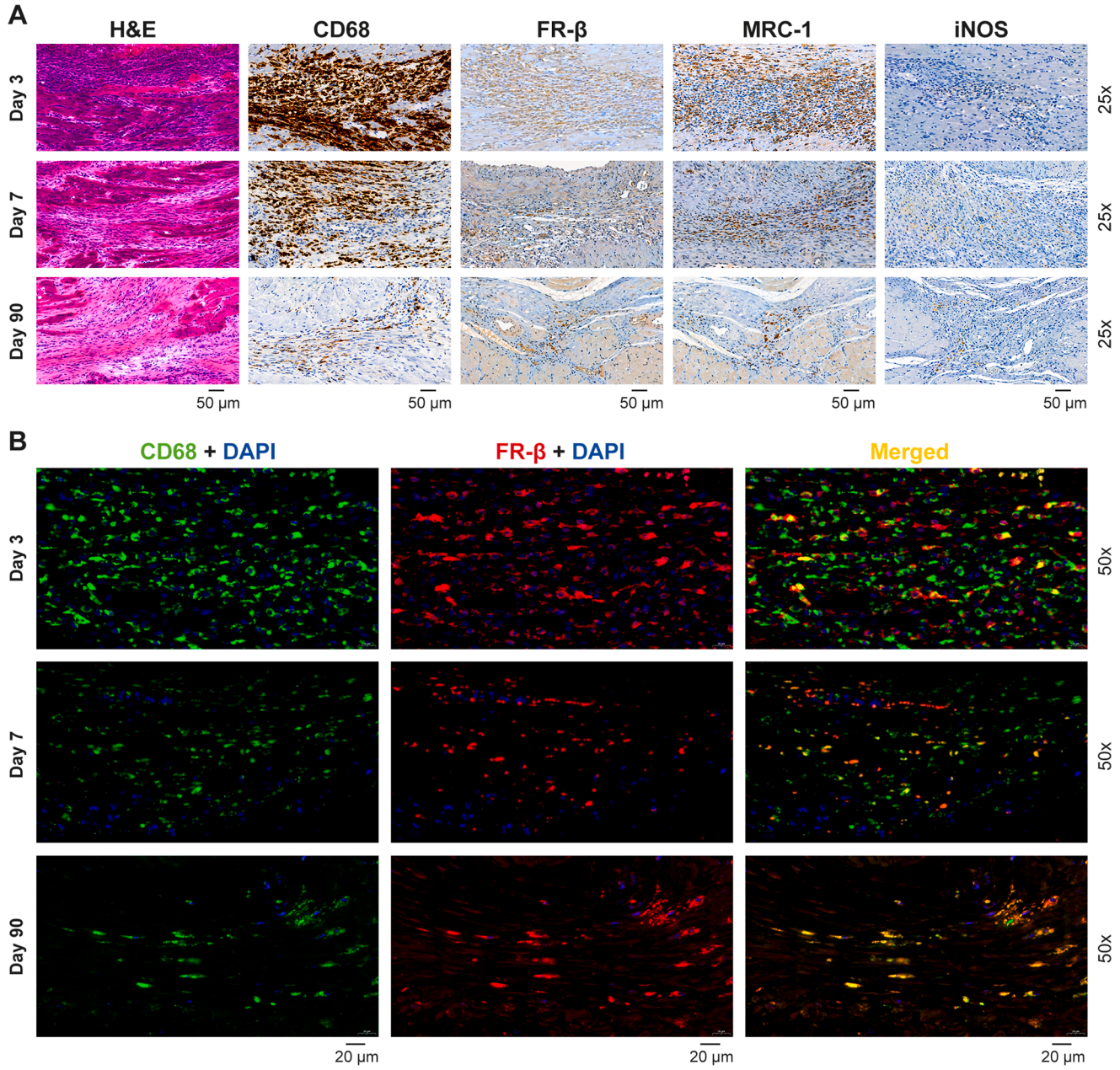

Figure 2. Detection of macrophages and FR-β. (A) High magnification microscopic images of infarct area in tissue sections stained with H&E and immunohistochemistry with antibodies against CD68, FR-β, MRC-1, and iNOS on days 3, 7, and 90 after MI. (B) Double immunofluorescence show nuclei (DAPI, blue), CD68-positive macrophages (green), and FR-β-positive macrophages (red). Merged image shows FR-β on a subset of CD68-positive macrophages (yellow).

infarct area (Figure 3 & Supplementary Fig. 2), whereas sham-operated rats showed low [^{18}F]FOL signal throughout the myocardium. Quantitative results of [^{18}F]FOL PET are shown in Figure 4 and Table 1. The uptake of [^{18}F]FOL in the infarct area peaked on day 3, when it was 2.7-fold higher than in the myocardium of sham-operated rats ($P < 0.001$). On days 7, 15, and 90, the uptake of [^{18}F]FOL remained 1.9-2.1-fold higher than in sham-operated rats ($P < 0.001$), but lower than on day 3 ($P < 0.001$ vs day 3, $P = 0.780$ day 7 vs day 15, $P = 0.973$ day 15 vs day 90). In the remote myocardium of the rats with MI, the uptake of [^{18}F]FOL was lower than in the infarct area at all time-points ($P < 0.001$), but showed a transient increase on day 3 as compared to sham-operated rats ($P = 0.027$). The uptake of [^{18}F]FOL was higher in blood and lower in the lungs of MI rats

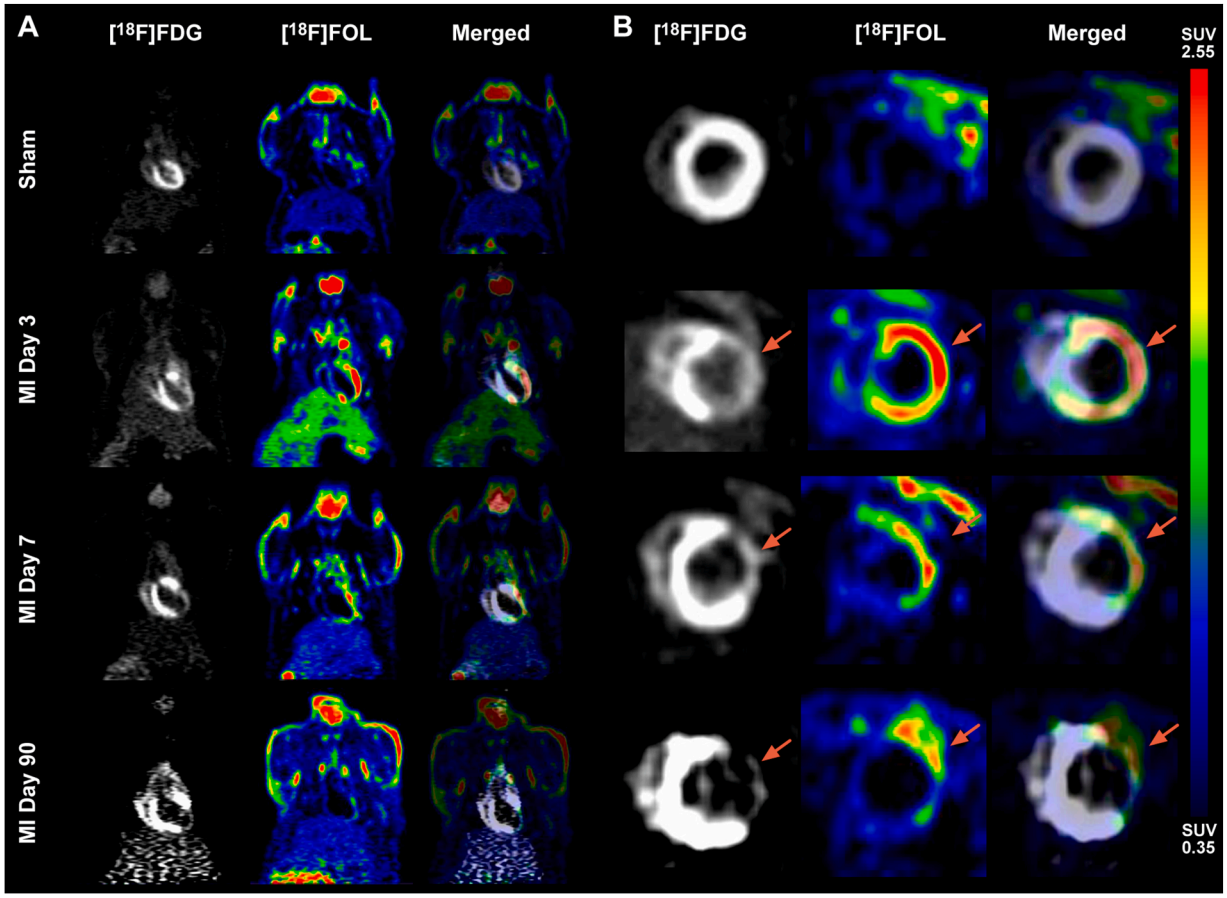

Figure 3. In vivo [^{18}F]FDG and [^{18}F]FOL PET images in rats after myocardial infarction (MI) on days 3, 7, and 90 or sham operation. Coronal plane (A) and cardiac short-axis (B) images showing infarct area with reduced uptake of [^{18}F]FDG in the anteriolateral wall of the LV (arrows). [^{18}F]FOL PET shows increased uptake of the tracer co-localizing with the infarct area that is discernible from the uptake in the chest wall wound area and adjacent organs.

compared to sham-operated on day 15 (Table 1). Time-activity curves (expressed as SUV) from a subset of rats that underwent dynamic PET imaging are shown in Supplementary Fig. 3.

Ex vivo autoradiography and biodistribution

Autoradiography demonstrated focally increased uptake of [^{18}F]FOL in the infarct area of rats with ligated LCA as compared to sham-operated rats or non-infarcted remote myocardium of rats with ligated LCA (Figures 1 and 4). In the infarct area, the uptake of [^{18}F]FOL peaked on day 3 ($P = 0.011$ vs day 7 and $P < 0.001$ vs day 90), when [^{18}F]FOL uptake also extended to adjacent non-infarcted regions. In comparison to sham-operated rats, the uptake in the infarct area was higher at all time-points ($P < 0.001$, Figure 4C, Table 2). In the remote myocardium, [^{18}F]FOL uptake was lower than in the infarct area at all time-points ($P < 0.001$ or $P = 0.001$), and showed an increase compared to sham-operated rats on day 90 ($P = 0.039$) post-MI (Figure 4D, Table 2).

Biodistribution of [^{18}F]FOL is summarized in Supplementary Table 2 showing the highest %ID/g in the kidneys and urine. On day 3, tracer accumulation in lungs, pancreas, bone, bone marrow, and urine was significantly higher in rats with MI than in sham-operated rats.

Effect of folate glucosamine on [^{18}F]FOL uptake

After the pre-injection of folate glucosamine, the [^{18}F]FOL uptake was decreased in the infarct area of LCA-ligated rats on day 3 post-MI (Tables 1 and 2, Supplementary Fig. 4). Compared to rats without pre-injection, the uptake of [^{18}F]FOL in the infarct area was 52.4% ($P = 0.002$) and 49.0% ($P = 0.026$) lower after the pre-injection as assessed by PET and autoradiography, respectively. In the remote myocardium, pre-injection had no effect on uptake of [^{18}F]FOL.

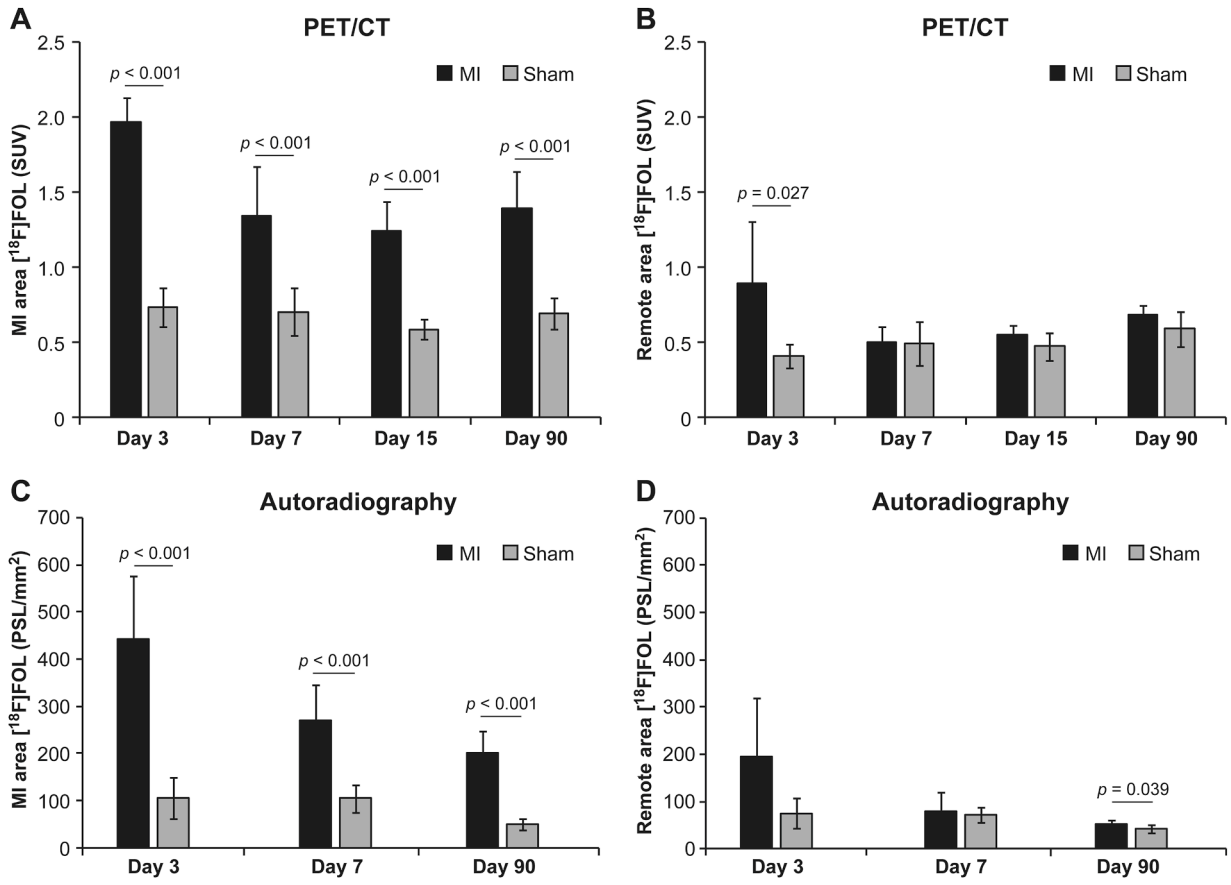

Figure 4. [^{18}F]FOL uptake in infarct and remote areas in rats with myocardial infarction (MI) or sham-operation 3, 7, 15, and 90 days after surgery as measured in vivo by PET (A, B) and ex vivo by autoradiography (C, D) on day 3, 7, and 90. Numbers of animals are shown in Supplementary Table 1. SUV, standardized uptake value; PSL/mm^2, photostimulated luminescence per square millimeter.

Table 1. [^{18}F]FOL uptake in different organs measured in vivo by PET

		Infarct area	Remote area	Blood	Liver	Lungs	Chest wall wound
Day 3	MI	1.97 ± 0.17	0.89 ± 0.41	0.44 ± 0.25	1.27 ± 0.48	0.35 ± 0.11	2.55 ± 0.51
	Sham	0.74 ± 0.13	0.41 ± 0.08	0.34 ± 0.12	0.75 ± 0.23	0.27 ± 0.05	2.15 ± 0.24
	P-value (MI vs Sham)	<0.001	0.027	0.428	0.051	0.154	0.145
Day 7	MI	1.35 ± 0.33	0.50 ± 0.11	0.37 ± 0.12	0.82 ± 0.16	0.30 ± 0.10	2.69 ± 0.43
	Sham	0.70 ± 0.16	0.49 ± 0.14	0.29 ± 0.12	0.82 ± 0.22	0.27 ± 0.09	2.71 ± 0.52
	P-value (MI vs Sham)	<0.001	0.818	0.065	0.925	0.353	0.896
Day 15	MI	1.24 ± 0.20	0.55 ± 0.06	0.43 ± 0.08	0.94 ± 0.15	0.25 ± 0.05	2.67 ± 0.21
	Sham	0.59 ± 0.07	0.47 ± 0.09	0.33 ± 0.05	0.86 ± 0.14	0.32 ± 0.03	2.58 ± 0.35
	P-value (MI vs Sham)	<0.001	0.113	0.046	0.406	0.028	0.602
Day 90	MI	1.39 ± 0.25	0.68 ± 0.07	0.35 ± 0.04	1.23 ± 0.28	0.33 ± 0.04	1.77 ± 0.75
	Sham	0.69 ± 0.11	0.59 ± 0.12	0.36 ± 0.04	1.05 ± 0.21	0.35 ± 0.10	2.11 ± 0.60
	P-value (MI vs Sham)	<0.001	0.055	0.631	0.162	0.602	0.327
Day 3	MI blocked[a]	1.03 ± 0.37	0.50 ± 0.02	0.45 ± 0.07	0.68 ± 0.03	0.32 ± 0.02	1.99 ± 0.03
	P-value (MI vs MI blocked)	0.002	0.186	0.977	0.100	0.643	0.224

Results are expressed as SUV. *MI*, myocardial infarction induced by left coronary artery ligation; *PET*, positron emission tomography; *Sham*, sham-operation.

[a] Rats were pre-injected with 100-fold molar excess of folate glucosamine to block the [^{18}F]FOL uptake.

Table 2. [^{18}F]FOL uptake in left ventricular myocardium measured ex vivo by autoradiography

	Day 3		Day 7		Day 90	
	Infarct area	Remote area	Infarct area	Remote area	Infarct area	Remote area
MI	441.27 ± 136.22	195.59 ± 122.73	270.85 ± 75.33	78.94 ± 40.33	201.03 ± 44.88	52.53 ± 9.24
Sham	105.37 ± 42.80	74.81 ± 31.61	104.09 ± 28.91	71.23 ± 16.28	49.64 ± 11.91	42.44 ± 9.16
P-value (MI vs Sham)	<0.001	0.059	<0.001	0.678	<0.001	0.039
MI, blocked[a]	216.12 ± 69.48	53.92 ± 16.80	ND	ND	ND	ND
P-value (MI vs MI blocked)	<0.05	0.074	ND	ND	ND	ND

Results are expressed as photostimulated luminescence per square millimeter. *MI*, myocardial infarction; *ND*, not determined; *Sham*, sham-operation.
[a] Rats were pre-injected with 100-fold molar excess of folate glucosamine to block the [^{18}F]FOL uptake.

Relationship between [^{18}F]FOL uptake and amount of CD68-positive macrophages

There was a positive correlation ($r = 0.669$, $P < 0.001$) between the uptake of [^{18}F]FOL by PET and area percentage of CD68 staining in the infarct area (Figure 5A) with combined data on day 3, 7, and 90 post-MI.

Relationship between [^{18}F]FOL uptake and LV function

The relationship between the uptake of [^{18}F]FOL and LV function was studied in 15 rats with MI (average MI size 27% ± 6.5% on day 7) and 5 sham-operated rats. As shown in Supplementary Table 4, echocardiography showed reduced LVEF as well as enlarged LV end-diastolic and end-systolic volumes in rats with MI versus sham operation on days 7, 15, and 90. Furthermore, LVEF was significantly lower on day 90 than day 7 post-MI ($P = 0.012$).

On day 7, the uptake of [^{18}F]FOL in the infarct area correlated negatively with LVDvol(i) ($r = -0.578$, $P = 0.024$), but not with LVEF ($r = 0.032$, $P = 0.908$), LVSvol(i) ($r = 0.444$, $P = 0.097$) or MI size ($r = -0.268$, $P = 0.335$) (Supplementary Fig. 5).

The uptake of [^{18}F]FOL in the infarct area on day 7 correlated with decline of LVEF from day 7 to day 90 post-MI ($r = -0.665$, $P = 0.007$) and enlargement of both LVDvol(i) ($r = 0.454$, $P = 0.089$) and LVSvol(i) ($r = 0.561$, $P = 0.029$, Figure 5) from day 7 to day 90 post-MI. When both [^{18}F]FOL uptake and MI size were included in the model, the uptake of [^{18}F]FOL remained a predictor of change in LVEF, whereas MI size did not ($P = 0.006$ and $P = 0.346$, respectively). Moreover, [^{18}F]FOL uptake in the remote area on day 7 significantly correlated with changes in LVEF, LVDvol(i), and LVSvol(i) from day 7 to day 90 post-MI (Figure 5).

DISCUSSION

The present study demonstrates the feasibility of imaging myocardial inflammatory response post-MI with the use of [^{18}F]FOL PET targeting FR-β, a marker of activated macrophages. The [^{18}F]FOL signal peaked on day 3 post-MI in both the infarcted and remote areas and remained elevated at a lower level until day 90 in the infarct area. Uptake of [^{18}F]FOL showed specificity for FR-β and correlated with the amount of CD68-positive macrophages in the infarcted area. Increased FR-β expression in the MI area and remote area early post-MI was associated with LV dilatation and decline of LV systolic function between 7 and 90 days post-MI. These results indicate that [^{18}F]FOL PET can be used to study myocardial inflammatory response after MI in vivo, detecting activated macrophages associated with long-term LV functional outcome post-MI.

The finding that expression of functional FR-β is strongly induced on activated macrophages, but not resting macrophages or other non-immune cell types in the setting of inflammatory response post-MI, has provided the rationale for investigating FR-β-targeted diagnostic tools and therapeutic intervention in inflammatory diseases [6,7,16,17]. Folate-based radiotracers have been evaluated for the imaging of activated macrophages in various inflammatory conditions, and exploratory clinical trials have shown accumulation of FR-β-targeting radiotracers in arthritic joints [18–20]. One study found folate-conjugated porphyrin nanoparticles to accumulate in infarcted myocardium 7 days post-MI in a mouse model, but the composition of the imaging agent did not allow for in vivo detection [21]. Previously, we found increased [^{18}F]FOL signal 1 and 2 weeks post-MI in a rat model [13]. Thus, we set out to evaluate [^{18}F]FOL in MI in more detail.

We found that [^{18}F]FOL enabled in vivo detection of FR-β-expressing macrophages in the myocardium at different time-points post-MI. Autoradiography confirmed increased [^{18}F]FOL PET signal in the macrophage-rich infarcted area, extending to adjacent non-infarcted myocardium on day 3. Furthermore, pre-treatment with folate

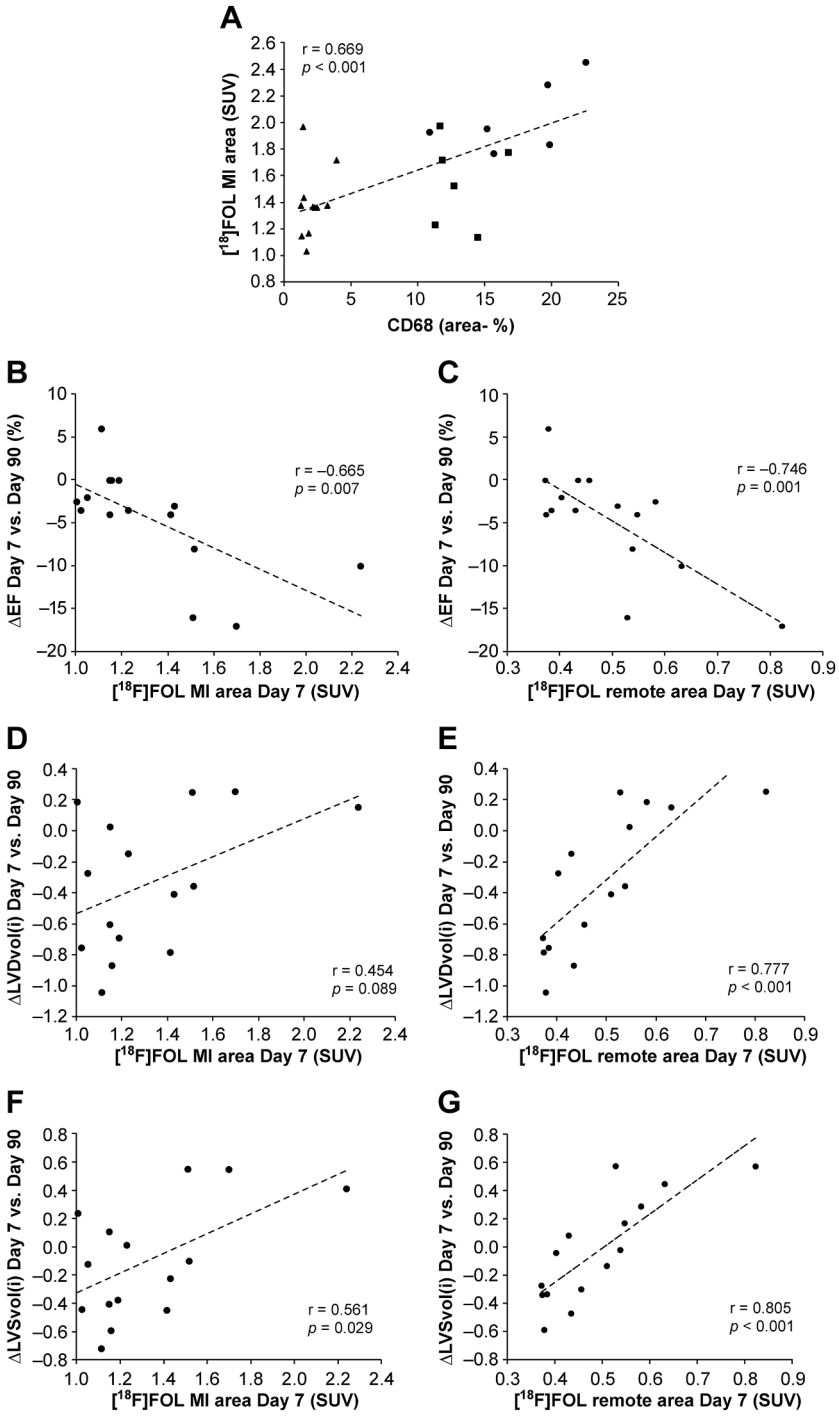

Figure 5. Scatterplots demonstrate correlations between [^{18}F]FOL uptake, area percentage of CD68, and long-term echocardiographic measures of LV function and size. (A) There was a positive correlation between [^{18}F]FOL uptake and area percentage of CD68-positive macrophages (circles = day 3, boxes = day 7, triangles = day 90). The uptake of [^{18}F]FOL in infarct (MI) area (B, D and F) and remote area (C, E and G) on day 7 correlates inversely with change in LV ejection fraction (ΔEF) over 90 days post-MI, and positively with changes in LV diastolic and systolic volumes indexed to body weight (ΔLVDvol(i) and ΔLVSvol(i), respectively) over 90 days post-MI.

glucosamine reduced the signal confirming specificity of the [^{18}F]FOL. Imaging probes targeting cell surface markers of different leukocyte subpopulations present the opportunity to visualize and quantify distinct phases of cardiac inflammation [9]. Our results are in line with previous studies demonstrating imaging of inflammatory response post-MI using [^{18}F]FDG and other PET tracers targeting chemokine receptors CXCR4 or CCR2, amino acid methionine metabolism [22], somatostatin receptors [23], the mitochondrial 18-kD translocator protein TSPO

[24,25], and mannose receptor [26,27]. The PET signal of [^{18}F]FOL appeared similar to the signal obtained with CCR2-or CXR4-targeted tracers (target-to-background ratios between 2 and 3) [28,29], exceeding that seen with tracers targeting somatostatin receptors or TSPO [23,24]. The signal of [^{18}F]FOL was specific to the inflamed area and not affected by uptake in the remote myocardium, which can be seen with tracers dependent on metabolism, such as [^{18}F]FDG, and TSPO-targeting tracers [9].

Macrophages express FR-β upon activation by pro-inflammatory factors [8,16], and FR-β-positive macrophages both express pro-inflammatory markers and secrete pro-inflammatory mediators, such as reactive oxygen species and TNF-alpha [8]. In line with this, we found that the uptake of [^{18}F]FOL both in the infarcted and remote area peaked early post-MI on day 3, coinciding with the peak in accumulation of pro-inflammatory monocytes [2] and the highest number of CD68-positive macrophages. The FR-β begins to be expressed in monocytes within the bone marrow; however, in the hematopoietic stage the cells are unable to internalize the receptor to facilitate the transport of the folic acid. After the maturation, the monocytes differentiating into macrophages with persistant FR-β play a key role in early inflammatory response, whereas the expression of CD68 is predominantly upregulated only after the macrophages are exposed to the inflammatory microenvironment [30,31]. This different timing of the expression of these two molecules in two distinct subgroups of macrophages may explain why colocalization of FR-β expression with CD68-positive cells and correlation of [^{18}F]FOL uptake and the amount of CD68 positivity were only partial early post-MI. Notably, there was a trend towards transient increase in [^{18}F]FOL accumulation in lymphoid organs, including the spleen, bone, and bone marrow on day 3 post-MI possibly related to systemic inflammatory response that warrants further investigation [23,28]. After day 3, [^{18}F]FOL PET signal remained increased in the infarct area, which may indicate either continuous recruitment of pro-inflammatory macrophages or continuous expression of FR-β in macrophage subsets expressing anti-inflammatory macrophage phenotype markers after the initial pro-inflammatory phase of MI [1,32]. The detection of FR-β expressing macrophages months after MI has potential implications in long-term cardiac remodeling and heart failure [1]. Similar to our findings, uptake of ^{68}Ga-DOTATATE, targeting somatostatin receptor subtype-2, was observed several months after human MI indicating ongoing myocardial inflammation [23]. Considering these evidences and the fact that FR-β is selectively expressed on the activated macrophages, our results indicate that [^{18}F]FOL PET can detect pro-inflammatory macrophages in the myocardium at different time-points post-MI.

Prolonged and excessive inflammatory responses after MI have been associated with impaired wound healing, larger infarct size, and worse contractile function [9,28]. We therefore examined whether early [^{18}F]FOL uptake at day 7 is associated with LV structure and function at 3 months. High [^{18}F]FOL uptake in the infarct area was associated with a decline in LVEF between days 7 and 90 and remained an independent predictor after adjustment for infarct size, which alone did not predict LVEF decline. Moreover, [^{18}F]FOL uptake in the remote myocardium correlated with LVEF decline and showed even stronger associations with increases in LV diastolic and systolic volumes than uptake in the infarct area. Together, these findings support the concept that FR-β expressing macrophage activity in both infarcted and remote myocardium is associated with adverse post-MI remodeling and functional outcomes and may represent a marker of maladaptive inflammatory responses.

Our results are consistent with previous findings that pro-inflammatory imaging markers, including [^{18}F]FDG [10], CXCR4 [28,33], CCR2 [29], and TSPO [24], were associated with worsened LV function after experimental or human MI. Molecular imaging of the inflammatory response to injury may provide an opportunity for guidance of targeted immunomodulatory interventions [9]. In an experimental study, a CXCR4-targeted imaging signal was used to identify optimal timing and candidates for treatment with a CXCR4-blocking drug, which subsequently improved contractile function only when PET indicated high expression of the CXCR4 target in myocardial tissue [28]. FR-β may be used as a route to deliver anti-folates specifically to activated macrophages [34]. Upon availability, such therapies could be tested in combination with [^{18}F]FOL PET post-MI.

Due to inherent differences between rat and human, our results cannot be directly translated to clinical setting. Small size of the rat heart may result in partial volume and spillover effects, which cannot be reliably addressed. More detailed analysis of macrophage subset

expressing FR-β would be of interest in future studies. In order to study relationship between [^{18}F]FOL uptake and LV dysfunction, we used a model of permanent coronary ligation resulting in large MI size, whereas time course and intensity of the signal may not be generalizable to setting of ischemia-reperfusion injury, which is clinically relevant in reperfused acute MI.

CONCLUSION

Cardiac [^{18}F]FOL PET detects increased expression of FR-β, a marker of activated macrophages after MI in a rat model. FR-β expression peaks early and remains elevated up to 3 months in the infarcted area. Increased FR-β expression early post-MI is associated with worsening of left ventricular systolic function.

NEW KNOWLEDGE GAINED AND CLINICAL IMPLICATIONS

What is new?

- Present study demonstrates that [^{18}F]FOL PET targeting FR-β expressed on activated macrophages detects both early and long-term phases of inflammation post-MI in a rat model.
- The uptake of [^{18}F]FOL early after MI was associated with deterioration of LV function late after MI.

What are clinical implications?

- [^{18}F]FOL PET is a potential approach for detection and monitoring of activated macrophages associated with LV dysfunction after MI.

FUNDING AND SUPPORT

This work was supported by grants from the Research Council of Finland (350117 and 343152), the Research Council of Finland's Flagship In-FLAMES (337530 and 357910), the Sigrid Jusélius Foundation, the Finnish Foundation for Cardiovascular Research, Finnish Cultural Foundation, the Jane and Aatos Erkko Foundation, and Finnish State Research Funding. Imran Iqbal is a PhD student partially supported by the Doctoral Programme in Clinical Research of the University of Turku Graduate School.

DISCLOSURES

Imran Iqbal PharmD, M.Sc: No conflicts of interest to disclose. **Heidi Liljenbäck** M.Sc; No conflicts of interest to disclose. **Putri Andriana** B.Pharm, M.Sc: No conflicts of interest to disclose. **Mia Ståhle** PhD: No conflicts of interest to disclose. **Jenni Virta** PhD: No conflicts of interest to disclose. **Erika Atencio Herre** M.Sc: No conflicts of interest to disclose. **Maxwell W.G. Miner** PhD: No conflicts of interest to disclose. **Arman Anand** MBBS, M.Sc: No conflicts of interest to disclose. **Aino Suni** MSc: No conflicts of interest to disclose. **Wail Nammas** M.D: No conflicts of interest to disclose. **Ville Kytö** MD, PhD: No conflicts of interest to disclose. **Hasan Mansour A Mansour** BSc: No conflicts of interest to disclose. **Nathan A. Cleveland** BSc: No conflicts of interest to disclose. **Xiang-Guo Li** PhD: No conflicts of interest to disclose. **Madduri Srinivasarao** PhD: No conflicts of interest to disclose. **Philip S. Low** PhD: No conflicts of interest to disclose. **Juhani Knuuti** MD, PhD: Dr. Knuuti declares consultancy fees from GE Healthcare and Synektik and speaker fees from Siemens (not related to the current study). **Anne Roivainen** PhD: No conflicts of interest to disclose. **Antti Saraste MD**, PhD: Dr. Saraste declares fees for lectures or consultation from Abbot, AstraZeneca, BMS, Janssen, Novo Nordisk, and Pfizer (not related to the current study).

ACKNOWLEDGMENTS

We thank Aake Honkaniemi for providing assistance with the PET studies and Marja-Riitta Kajaala and Erica Nyman (Histology core facility, Institute of Biomedicine, University of Turku, Finland) for tissue sectioning and immunostaining and Timo Kattelus for processing the figures.

APPENDIX A. SUPPLEMENTARY DATA

Supplementary data to this article can be found online at https://doi.org/10.1016/j.nuclcard.2026.102653.

REFERENCES

[1] Prabhu SD, Frangogiannis NG. The biological basis for cardiac repair after myocardial infarction. Circ Res 2016;119:91–112. https://www.ahajournals.org/doi/abs/10.1161/CIRCRESAHA.116.303577.

[2] Nahrendorf M, Swirski FK, Aikawa E, Stangenberg L, Wurdinger T, Figueiredo JL, et al. The healing myocardium sequentially mobilizes two monocyte subsets with divergent and complementary functions. J Exp Med 2007;204:3037–47. https://doi.org/10.1084/jem.20070885.

[3] Frantz S, Hundertmark MJ, Schulz-Menger J, Bengel FM, Bauersachs J. Left ventricular remodelling post-myocardial infarction: pathophysiology, imaging, and novel therapies. Eur Heart J 2022;43:2549–61. https://doi.org/10.1093/eurheartj/ehac223.

[4] Kubota A, Frangogiannis NG. Macrophages in myocardial infarction. Am J Physiol Cell Physiol 2022;323:C1304–24. https://doi.org/10.1152/ajpcell.00230.2022.

[5] Nahrendorf M. Myeloid cells in cardiovascular organs. J Intern Med 2019;285:491–502. https://doi.org/10.1111/joim.12844.

[6] Nakashima-Matsushita N, Homma T, Yu SU, Matsuda T, Sunahara N, Nakamura T, et al. Selective expression of folate receptor and its possible role in methotrexate transport in synovial macrophages from patients with rheumatoid arthritis. Arthritis Rheum 1999;42:1609–16. 10.10021529-0131(199908)42:8<1609::AID-ANR7>3.0CO;2-L.

[7] Van Der Heijden JW, Oerlemans R, Dijkmans BAC, Qi H, Van Der Laken CJ, Lems WF, et al. Folate receptor β as a potential delivery route for novel folate antagonists to macrophages in the synovial tissue of rheumatoid arthritis patients. Arthritis Rheum 2009;60:12–21. https://doi.org/10.1002/art.24219.

[8] Xia W, Hilgenbrink AR, Matteson EL, Lockwood MB, Cheng JX, Low PS. A functional folate receptor is induced during macrophage activation and can be used to target drugs to activated macrophages. Blood 2009;113:438–46. https://doi.org/10.1182/blood-2008-04-150789.

[9] Thackeray JT, Lavine KJ, Liu Y. Imaging inflammation past, present, and future: focus on cardioimmunology. J Nucl Med 2023;64:39S–48S. https://doi.org/10.2967/jnumed.122.264865.

[10] Jahandideh A, Uotila S, Ståhle M, Virta J, Li XG, Kytö V, et al. Folate receptor β–Targeted PET imaging of macrophages in autoimmune myocarditis. J Nucl Med 2020;61:1643–9. https://doi.org/10.2967/jnumed.119.241356.

[11] Silvola JMU, Li XG, Virta J, Marjamäki P, Liljenbäck H, Hytönen JP, et al. Aluminum fluoride-18 labeled folate enables in vivo detection of atherosclerotic plaque inflammation by positron emission tomography. Sci Rep 2018;8:9720. https://doi.org/10.1038/s41598-018-27618-4.

[12] Elo P, Li XG, Liljenbäck H, Helin S, Teuho J, Koskensalo K, et al. Folate receptor-targeted positron emission tomography of experimental autoimmune encephalomyelitis in rats. J Neuroinflammation 2019;16:1–18. https://doi.org/10.1186/s12974-019-1612-3.

[13] Torrieri G, Iqbal I, Fontana F, Talman V, Liljenbäck H, Putri A, et al. Macrophage hitchhiking nanoparticles for the treatment of myocardial infarction: an in vitro and in vivo study. Adv Funct Mater 2023;33:2303658. https://doi.org/10.1002/adfm.202303658.

[14] Kiugel M, Dijkgraaf I, Kytö V, Helin S, Liljenbäck H, Saanijoki T, et al. Dimeric [^{68}Ga]DOTA-RGD peptide targeting αvβ3 integrin reveals extracellular matrix alterations after myocardial infarction. Mol Imag Biol 2014;16:793–801. https://doi.org/10.1007/s11307-014-0752-1.

[15] Ståhle M, Kytö V, Kiugel M, Liljenbäck H, Metsälä O, Käkelä M, et al. Glucagon-like peptide-1 receptor expression after myocardial infarction: imaging study using ^{68}Ga-NODAGA-exendin-4 positron emission tomography. J Nucl Cardiol 2018;27:2386–97. https://doi.org/10.1007/s12350-018-01547-1.

[16] Paulos CM, Turk MJ, Breur GJ, Low PS. Folate receptor-mediated targeting of therapeutic and imaging agents to activated macrophages in rheumatoid arthritis. Adv Drug Deliv Rev 2004;56:1205–17. https://doi.org/10.1016/j.addr.2004.01.012.

[17] Hu Y, Wang B, Shen J, Low SA, Putt KS, Niessen HWM, et al. Depletion of activated macrophages with a folate receptor-beta-specific antibody improves symptoms in mouse models of rheumatoid arthritis. Arthritis Res Ther 2019;21:43. https://doi.org/10.11186/s13075-019-1912-0.

[18] Kraus VB, McDaniel G, Huebner JL, Stabler TV, Pieper CF, Shipes SW, et al. Direct in vivo evidence of activated macrophages in human osteoarthritis. Osteoarthr Cartil 2016;24:1613–21. https://doi.org/10.1016/j.joca.2016.04.010.

[19] Verweij NJF, Yaqub M, Bruijnen STG, Pieplenbosch S, ter Wee MM, Jansen G, et al. First in man study of [^{18}F]fluoro-PEG-folate PET: a novel macrophage imaging technique to visualize rheumatoid arthritis. Sci Rep 2020;10:1047, s41598-020-57841-x.

[20] Matteson EL, Lowe VJ, Prendergast FG, Crowson CS, Moder KG, Morgenstern DE, et al. Assessment of disease activity in rheumatoid arthritis using a novel folate targeted radiopharmaceutical folatescan. Clin Exp Rheumatol 2009;27:253 https://pmc.ncbi.nlm.nih.gov/articles/PMC4343259/.

[21] Ni NC, Jin CS, Cui L, Shao Z, Wu J, Li SH, et al. Non-invasive macrophage tracking using novel porphysome nanoparticles in the post-myocardial infarction murine heart. Mol Imag Biol 2016;18:557–68. https://doi.org/10.1007/s11307-015-0922-9.

[22] Thackeray JT, Bankstahl JP, Wang Y, Wollert KC, Bengel FM. Targeting amino acid metabolism for molecular imaging of inflammation early after myocardial infarction. Theranostics 2016;6:1768–79. https://doi.org/10.7150/thno.15929.

[23] Tarkin JM, Calcagno C, Dweck MR, Evans NR, Chowdhury MM, Gopalan D, et al. ^{68}Ga-DOTATATE PET identifies residual myocardial inflammation and bone marrow activation after myocardial infarction. J Am Coll Cardiol 2019;73:2489–91. https://doi.org/10.1016/j.jacc.2019.02.052.

[24] Thackeray JT, Hupe HC, Wang Y, Bankstahl JP, Berding G, Ross TL, et al. Myocardial inflammation predicts remodeling and neuroinflammation after myocardial infarction. J Am Coll Cardiol 2018;71:263–75. https://doi.org/10.1016/j.jacc.2017.11.024.

[25] MacAskill MG, Stadulyte A, Williams L, Morgan TEF, Sloan NL, Alcaide-Corral CJ, et al. Quantification of macrophage-driven inflammation during myocardial infarction with ^{18}F-LW223, a novel TSPO radiotracer with binding independent of the rs6971 human polymorphism. J Nucl Med 2021;62:536–44. https://doi.org/10.2967/jnumed.120.243600.

[26] Werner RA, Thackeray JT, Diekmann J, Weiberg D, Bauersachs J, Bengel FM. The changing face of nuclear cardiology: guiding cardiovascular care toward molecular medicine. J Nucl Med 2020;61:951–61. https://doi.org/10.2967/jnumed.119.240440.

[27] Varasteh Z, Braeuer M, Mohanta S, Steinsiek AL, Habenicht A, Omidvari N, et al. In vivo visualization of M2 macrophages in the myocardium after myocardial infarction (MI) using ^{68}Ga-NOTA-Anti-MMR nb: targeting mannose receptor (MR, CD206) on M2 macrophages. Front Cardiovasc Med 2022;9:889963. https://doi.org/10.3389/fcvm.2022.889963.

[28] Hess A, Derlin T, Koenig T, Diekmann J, Wittneben A, Wang Y, et al. Molecular imaging-guided repair after acute myocardial infarction by targeting the chemokine

receptor CXCR4. Eur Heart J 2020;41:3564–75. https://doi.org/10.1093/eurheartj/ehaa598.

[29] Heo GS, Kopecky B, Sultan D, Ou M, Feng G, Bajpai G, et al. Molecular imaging visualizes recruitment of inflammatory monocytes and macrophages to the injured heart. Circ Res 2019;124:881–90. https://doi.org/10.1161/CIRCRESAHA.118.314030.

[30] Reddy JA, Haneline LS, Srour EF, Antony AC, Clapp DW, Low PS. Expression and functional characterization of the β-Isoform of the folate receptor on CD34+ cells. Blood 1999;93:3940–8. https://doi.org/10.1182/blood.V93.11.3940.

[31] Ramprasad MP, Terpstra V, Kondratenko N, Quehenberger O, Steinberg D. Cell surface expression of mouse macrosialin and human CD68 and their role as macrophage receptors for oxidized low density lipoprotein. Proc Natl Acad Sci USA 1996;93:14833–8. https://doi.org/10.1073/pnas.93.25.14833.

[32] Warmink K, Siebelt M, Low PS, Riemers FM, Wang B, Plomp SGM, et al. Folate receptor expression by human monocyte–derived macrophage subtypes and effects of corticosteroids. Cartilage 2022;13:19476035221081469. https://doi.org/10.1177/19476035221081469.

[33] Werner RA, Koenig T, Diekmann J, Haghikia A, Derlin T, Thackeray JT, et al. CXCR4-Targeted imaging of post-infarct myocardial tissue inflammation: prognostic value after reperfused myocardial infarction. JACC Cardiovasc Imaging 2022;15:372–4. https://doi.org/10.1016/j.jcmg.2021.08.013.

[34] Lu Y, Stinnette TW, Westrick E, Klein PJ, Gehrke MA, Cross VA, et al. Treatment of experimental adjuvant arthritis with a novel folate receptor-targeted folic acid-aminopterin conjugate. Arthritis Res Ther 2011;13:R56. https://doi.org/10.1186/ar3304.